HHS Public Access

Author manuscript

J Neurochem. Author manuscript; available in PMC 2017 April 01.

Published in final edited form as:

J Neurochem. 2016 April ; 137(2): 253–265. doi:10.1111/jnc.13536.

Calpastatin inhibits motor neuron death and increases survival of hSOD1^{G93A} mice

Mala V Rao[1,2,*], **Jabbar Campbell**[1], **Arti Palaniappan**[1], **Asok Kumar**[1,3], and **Ralph A Nixon**[1,2,4]

[1]Nathan Kline Institute, 140 Old Orangeburg Road, Orangeburg, NY 10962

[2]Department of Psychiatry, Langone Medical Center, NYU School of Medicine, New York, NY 10016

[3]Department of Pathology, Langone Medical Center, NYU School of Medicine, New York, NY 10016

[4]Department of Cell Biology, Langone Medical Center, NYU School of Medicine, New York, NY 10016

Abstract

Amyotrophic lateral sclerosis (ALS) is a progressive motor neuron disease with a poorly understood cause and no effective treatment. Given that calpains mediate neurodegeneration in other pathological states and are abnormally activated in ALS, we investigated the possible ameliorative effects of inhibiting calpain overactivation in hSOD1^{G93A} transgenic (Tg) mice in vivo by neuron specific overexpression of calpastatin (CAST), the highly selective endogenous inhibitor of calpains. Our data indicate that overexpression of CAST in hSOD1^{G93A} mice, which lowered calpain activation to levels comparable to WT mice, inhibited the abnormal breakdown of cytoskeletal proteins (spectrin, MAP2 and neurofilaments), and ameliorated motor axon loss. Disease onset in hSOD1^{G93A}/CAST mice compared to littermate hSOD1^{G93A} mice is delayed, which accounts for their longer time of survival. We also find that neuronal overexpression of CAST in hSOD1^{G93A} transgenic mice inhibited production of putative neurotoxic caspase-cleaved tau and activation of Cdk5, which have been implicated in neurodegeneration in ALS models, and also reduced the formation of SOD1 oligomers. Our data indicate that inhibition of calpain with CAST is neuroprotective in an ALS mouse model.

[*]Address to correspondence: Dr. Mala V. Rao, Nathan Kline Institute, 140 Old Orangeburg Road, Orangeburg, NY 10962. Ph: 845 398 5547; Fax: 845 398 5422; rao@nki.rfmh.org.

Author Contributions:

MVR designed the research; MVR, JC, AP, and AK performed the experiments; MVR and RAN interpreted the data and wrote the paper.

Conflicts of interest: “none”

Potential Conflict of Interest:

The authors declare that there are no competing financial interests. Authors also state that this study does not involve any commercial sponsor of any diagnostic or treatment method that is used in the manuscript. The study was funded by NIH/NINDS/NIA (see acknowledgement section).

Keywords

Calpain; Caspase-3; neurofilament; oligomers; Transgenic mice; Spectrin

Introduction

ALS is a progressive motor neuron disease characterized by degeneration of motor neurons in spinal cord, brain stem and motor cortex and patients die within 3–5 yrs of disease onset with progressive muscle weakness, atrophy and spasticity (Ajroud-Driss & Siddique 2015). In 90% of cases, no genetic link (sporadic-ALS) is found while, in 10%, the disease is familial (F-ALS) and inherited mainly in a dominant fashion and these two forms of ALS are indistinguishable (Bruijn *et al.* 2004). Mutations in ~20 genes cause F-ALS, including superoxide dismutase 1 (SOD1), TAR DNA binding protein-43 (TDP-43), ubiquilin2, fused in sarcoma (FUS) or translocated in liposarcoma (TLS), and hexanucleotide repeat expansion in the intronic region of C9ORF72 (Ajroud-Driss & Siddique 2015). SOD1 and C9ORF72 mutations together account for at least 50% of reported F-ALS cases (Robberecht & Philips 2013, Ajroud-Driss & Siddique 2015).

SOD1, a 153 amino acid cytosolic antioxidant protein, involved in conversion of reactive oxygen into water in cells requires copper and zinc for activity (Bruijn *et al.* 2004, Rosen *et al.* 1993). More than 160 different mutations of SOD1 have been identified in ALS patients (Andersen & Al-Chalabi 2011) and misfolding of wild type SOD1 protein has also been identified in the motor neurons of “sporadic” ALS patients carrying no known causative mutations (Bosco *et al.* 2010). Transgenic mice with mutant human SOD1 (hSOD1) genes develop a motor neuron disease similar to ALS, whereas mice lacking SOD1 exhibit no disease symptoms (Ajroud-Driss & Siddique 2015, Bruijn *et al.* 2004, Reaume *et al.* 1996). Multiple hypotheses have been proposed to explain mutant SOD1-mediated motor neuron degeneration in ALS including SOD1 oligomerization, protein aggregate formation, mitochondrial dysfunction, glutamate-mediated excitotoxicity, axonal transport abnormalities, toxicity from non-neuronal neighboring cells, mutant SOD1 protein-mediated oxidative damage, altered autophagy, growth factor deficiency, and inflammation (Ajroud-Driss & Siddique 2015, Bruijn *et al.* 2004, Boillee *et al.* 2006, Nassif *et al.* 2014).

Although SOD1 mutations causative for ALS have been known for more than 20 years (Rosen *et al.* 1993), an effective therapy for ALS has remained elusive. The anti-glutamatargic agent riluzole is the only FDA approved drug for ALS patients (Doble 1996) and has marginal therapeutic efficacy by attenuating excitotoxicity-mediated motor neuron death. Excitotoxicity and altered calcium homeostasis in motor neurons of ALS patients (Van Den Bosch *et al.* 2006, Tadic *et al.* 2014) is associated with calpain over-activation and degradation of cytoskeletal proteins, such as neurofilaments (NFs), tau, and microtubule associate protein 2 (MAP2) (Rao *et al.* 2008, Rao *et al.* 2014, Ray *et al.* 2000). Calpains are neutral cysteine proteases involved in various cellular functions that require calcium for their activation (Goll *et al.* 2003, Nixon 2003). Calpains, encoded by multiple genes, are broadly categorized based on an *in vitro* calcium requirement in the μM range (calpain I or μ-calpain) or mM range (calpain II or m-calpain), each composed of an 80-kDa catalytic and a

28-kDa regulatory subunit (Goll *et al.* 2003). Calpains form a complex with CAST, the only known endogenous protein inhibitor of calpain activity in cells (Goll *et al.* 2003). CAST has 4 inhibitory domains, released after limited proteolysis by activated calpain and further cleaved and inactivated by calpains and caspases (Wang *et al.* 1998). CAST depletion in Alzheimer's disease, Parkinson's disease, Huntington's Disease and the tauopathy of Frontotemporal Dementia is associated with abnormal calpain activation and extensive neurofibrillary degeneration and restoration of CAST in mouse models of these diseases is therapeutic (Rao *et al.* 2008, Rao *et al.* 2014, Menzies *et al.* 2015, Diepenbroek *et al.* 2014). In light of the observations that calpains are activated in neuromuscular diseases (Spencer & Mellgren 2002, Wootz *et al.* 2006, Stifanese *et al.* 2014), we tested whether blocking calpain activation by elevating levels of the highly selective inhibitor CAST would have beneficial effects in a hSOD1^{G93A} mouse model of ALS. Our observations in this paper indicate that neuron specific overexpression of CAST in hSOD1^{G93A} mice inhibits calpain hyper-activation, abnormal activation of CDK5, cytoskeletal protein breakdown, SOD1 oligomer formation, increases motor axon survival, delays disease onset and prolongs the life of hSOD1^{G93A} mice.

Materials and Methods

Animals: heterozygous hSOD1^{G93A} low expression line of mice (SOD1*G93Adl) 1Gur (SOD1G93Adl; also known as G1del, has ~8 copies of transgene, Alexander *et al., 2004*) in C57BL/6J background (maintained for more than 9 generations, did not observe any genetic drift in these mice) are screened as described previously (Gurney *et al.* 1994). These low expression mice develop motor neuron disease at a slower rate and exhibit pathological changes that most closely resemble those in human ALS patients (Dal Canto & Gurney 1997). Heterozygous CAST transgenic mice maintained (for more than 9 generations) in C57BL/6J background are screened as previously described (Rao *et al.* 2008). Male hSOD1^{G93A} and female CAST Tg mice were bred to obtain WT, CAST, hSOD1^{G93A} and hSOD1^{G93A}/CAST mice in a 1:1:1:1 ratio, respectively, according to Mendelian genetics. Mice were maintained in a 12 hr dark and 12 hr light cycle at Nathan Kline Institute animal facility, in all the experiments, both female and male mice were used. All the animal protocols used in the study were approved by the Nathan Kline Institute IACUC and that all the studies were conducted in accordance with the United States Public Health Service's Policy on Humane Care and Use of Laboratory Animals.

Preparation of spinal cords extracts, SDS-PAGE and Western blotting: 3–9 month old mice spinal cords were homogenized in a buffer (50 mM Tris-HCl, pH 8.0, 150 mM NaCl, 50 EDTA, 1% glycerol, 1 mM β-glycerophosphate, 1 mM NaF, 0.2 mM $NaVaO_4$ and 0.1 mM PMSF) and centrifuged at 14,000*g* for 20' at 4°C, clear supernatants (20 μg) were immunoblotted with CAST [CAST 3.1, (Rao *et al.* 2008)], SOD1 (Sigma), NF-L (NR-4), NF-H polyclonal (Rao *et al.* 2014), Cal I polyclonal Ab (Ab28258, Abcam, Cambridge, MA), spectrin (mAb 1622), α-internexin (MAB5224), NF-M (RMO44-Zymed, CA), p35 (Cell Signaling, MA), MAP2 [18.1, (Rao *et al.* 2008)], TauC3, H-300 (CAST, Santa Cruz Biotech, CA) and actin (N-350, used as a loading control) antibodies, and developed with ECL reagent (Amersham reagent). Immunoreactive bands captured on X-ray films were quantified using Multi Gauage V2.3 software (Fuji film, Tokyo, Japan).

Immunocytochemistry and Immunoflurosence of Motor neurons: mice were transcardially perfused with 4% para-formaldehyde solution in phosphate buffer, spinal cord vibratome sections (L5 region, 40 μm) were immunostained with C-24, a cal II antibody (a conformation specific and active site targeted antibody: there are no comparable antibodies that detect activated calpain II by western blot analysis. The reverse situation is true for immunochemical detection of activated mouse calpain I) (Rao *et al.* 2008), washed, then incubated with biotinylated 2° antibody (anti-IgG) and finally incubated for 1 hr in an Avidin–biotin–peroxidase complex (ABC) solution (Vector Laboratories, CA). Then the sections were washed, incubated in a solution containing 0.1% 3, 39-diaminobenzidine (DAB; 50 mg/100 ml), and developed with H_2O_2 (0.02%). The sections were mounted onto gelatin-coated slides, cresyl violet stained, dehydrated through alcohol to xylene and images were captured on a light microscope as described previously (Rao *et al.* 2008). For immunofluorescence, spinal cord sections were incubated with CAST (3.1), and neurofilament middle molecular weight (NF-M, RMO44) or CAST 3.1 and GFAP, or CAST 3.1 and choline acetyl transferase (ChAT) antibodies and immunofluoresence analysis was carried out as described previously (Rao *et al.* 2008) and images were captured on Leica TCS-NT confocal microscope.

Morphometric analysis and motor axon counts

Mice at the ages of 3, 6 and 9 months were anesthetized, perfused transcardially with 4% paraformaldehyde, 2.5% glutaraldehyde, processed for electron microscopy as described previously (Rao *et al.* 2014) and semi-thick sections (0.75 μm) were imaged under light microscopy after toluidine blue stain. Axons were counted in L5 root cross sections and axon diameters from different genotypes and age groups of L5 ventral roots were measured using Integrated Morphometry analysis function from the Image 1/Metamorph Imaging system (Universal Imaging Corp., West Chester, PA) as described previously (Rao *et al.* 2014). Axons were divided into 2 groups (< 5 μm and > 5 μm) based on their sizes, axons bigger than 5 μm are degenerated in hSOD1 mutant mice and human ALS patients (Bruijn *et al.* 2004).

Disease onset, progression and survival measurements

Disease onset symptom measurements were performed as described previously (Rao *et al.* 2014). Briefly, each week animals over 4 months of age were held by their tail, and examined for deviation from the normal symmetrical slaying of the hind limbs. Hind limb dysfunction evidenced by folding one or both of their legs or clasping them together was considered “disease onset”. The interval from the time of birth to the disease onset was considered time of “disease onset”. The interval from time of disease onset to the death of the animal was considered “disease duration or progression”. The interval from the birth to death of the animal was considered “survival” time period. “End stage” is defined as the age at which the animal is unable to right itself in 30 sec when placed on its side.

Rotarod Tests

Mice were subject to accelerating Rotarod tests (Liu *et al.* 2012) (Ugo Basile, Comerio, Italy) at 3, 6 and 9 months of age with modifications. Briefly, mice were subjected to 3 trials with 45 min intertrial intervals before the test. Mice were placed on a stationary bar and

tested at an accelerating rate of 6 r.p.m. The total time from the start of the test to mice fall from the bar was recorded as an animal endurance time (AET) in seconds. Tests were stopped at 3.5 min for animals that remained on the bar. Three tests were conducted for each mouse with at least a 5-min rest in between each test. The average time from 3 tests were calculated and used for each data point. Rotarod measurements were performed by individuals who did not know the genotypes of the animals to avoid bias towards a particular genotype.

Statistical analysis

Both one way ANOVA followed by Bonferroni's multiple comparisons test, and Student's t-test analyses were used to assess significance of differences between samples. *p value <0.05 is significant; error bars indicate SEM in all figures.

Results

Calpain is over-activated in hSOD1^{G93A} Tg mice and associated with CAST depletion, cytoskeletal protein breakdown, and Cdk5 activation

An immunocytochemical analysis of the activated form of calpain II using a polyclonal antibody (C-24) directed against the active site of calpain II (Rao *et al.* 2008, Rao *et al.* 2014, Grynspan *et al.* 1997), revealed increased immunoreactivity in the cell bodies (see arrows) and neuronal processes (see arrow heads) of motor neurons in spinal cords of end stage (~9 month old) hSOD1^{G93A} mice (Fig. 1a), as compared to age matched controls. In immunoblot analyses with a calpain I-specific antibody that recognizes full-length and activated truncated calpain I isoforms (Thapa *et al.* 2012), we observed a lowered level of full length 80-kDa calpain I in spinal cord extracts from hSOD1^{G93A} mice compared to WT controls (Fig. 1b, see arrow). Notably, a 50-kDa immunoreactive band, known to be an activated form of calpain I was present in spinal cords of hSOD1^{G93A} mice but not in WT mice. Consistent with these findings, we observed significantly reduced levels of well-established calpain substrates, including calpastatin and MAP2 (Rao *et al.* 2008, Rao *et al.* 2014, Menzies *et al.* 2015, Diepenbroek *et al.* 2014). Calpain activation was further reflected by higher levels of a specific calpain-generated 150 kDa cleavage product of spectrin (Fig. 1c) (150-kDa spectrin BDP) (Rao *et al.* 2008, Rao *et al.* 2014), increased cleavage of the p35 form of cdk5 yielding the constitutively active p25 form known to be associated with protein hyperphosphorylation and neurodegeneration (Nguyen & Julien 2003). Consistent with earlier reports of elevated caspase-3 activity in hSOD1^{G93A} mice (Boston-Howes *et al.* 2006), caspase-3 activation, another known effect of activated calpain contributing to neurodegeneration, was evidenced by elevated levels of a specific caspase-generated 120 kDa cleavage product of spectrin (Fig. 1c). Caspase-3 activity also generates a specific tau cleavage product (TauC3) in human AD brains (Rao *et al.* 2008), and tauopathy models (Rao *et al.* 2014) and accordingly, we observed significantly increased TauC3 immunoreactivity in hSOD1^{G93A} spinal cords compared with WT extracts (Fig. 1c–d). Quantitative immunoblot analyses of these calpain substrates in hSOD1^{G93A} and WT mice confirmed substantially reduced levels of all four neurofilament subunit proteins (NFL, Neurofilament Light; NFM, Neurofilament Medium; NFH, Neurofilament Heavy, and α-internexin) (Rao *et al.* 2014), MAP2, and CAST (Fig. 1d). Moreover, levels of 150-kDa spectrin BDP (Fig. 1c, 1e, $p<0.05$,

Student's t-test) (Rao *et al.* 2008, Rao *et al.* 2014, Higuchi *et al.* 2012), 120-kDa caspase-3-cleaved spectrin (Fig. 1c, e, $p<0.05$), TauC3 reactive 50-kDa tau band (Fig 1c, 1e, $p<0.05$), p25 and the ratio of p25/p35 were significantly increased in hSOD1^{G93A} mice spinal cord extracts (Fig 1c, 1e, $p<0.05$, Student's t-test).

Recent studies indicate that SOD1 oligomers are neurotoxic (Liu *et al.* 2012) and that therapies directed toward eliminating monomeric/misfolded SOD1 and oligomeric SOD1 prevent neuronal cell death and prolong the lifespan of model mice (Liu *et al.* 2012). Immunoblot analyses using an SOD1 antibody that detects mouse and human SOD1, revealed a pattern of immunoreactive bands corresponding to SOD1 oligomers in the range of 30–300 kDa in size (see the arrows in Fig. 1c for SOD1 oligomers panel and Fig. 1e, $p<0.05$, Student's t-test), similar to that previously described (Liu *et al.* 2012).

To examine the point at which the calpain is activated in hSOD1^{G93A} mice, we performed quantitative immunoblot analysis of the spinal cord extracts of these mice at 3 and 5 months of age and find significantly increased levels of 150-kDa spectrin, and p25 (Fig. 1f–h, $p<0.05$, Student's t-test) which are markers of calpain activation (Rao et al., 2008' 2014; Goll et al., 2003) at these ages. These results suggest that calpain activation is an early event in this mouse model and it develops at least 3 months before the onset of behavioral/ neurological symptoms of the disease.

CAST overexpression blocks calpain-mediated cytoskeleton breakdown and CDK5 activation in hSOD1^{G93A} mice

The biochemical changes in hSOD1^{G93A} mice described above are a pattern seen in other neurodegenerative disorders (Rao *et al.* 2008, Rao *et al.* 2014, Menzies *et al.* 2015, Diepenbroek *et al.* 2014) and linked, at least in part, to calpain-mediated depletion of CAST. Accordingly, we investigated the pathogenic significance of calpain over-activation in hSOD1^{G93A} mice by determining whether or not restoring CAST levels is neuroprotective in this ALS model. We produced and previously characterized a line of transgenic mice expressing human CAST under the Thy-1.1 promoter to drive neuron specific expression at levels 10-fold higher than endogenous mouse CAST (Rao *et al.* 2008). To show that human CAST is also expressed in motor neurons, CAST mice spinal cords sections (cross and longitudinal) were double immunostained with CAST (3.1 antibody) (Rao *et al.* 2008), and a monoclonal NF-M antibody (RMO44) which immunolabels mainly axons and more weakly certain neuronal perikarya in WT mice. CAST strongly colocalized with NF-M in axons and was also detected in the cell bodies of motor neurons (Fig. 2a, see arrows for cell body and axonal compartments). By contrast, CAST (indicated with arrows in cell bodies and axons) did not immunocolocalize with glial fibrillary acidic protein, a marker of fibrous astrocytes, in double immunofluoresence analyses (Fig. 2a) confirming neuron-specific CAST expression (Rao *et al.* 2008, Rao *et al.* 2014). Our double immunofluorescence studies with CAST and motor neuron specific ChAT antibody reveal that CAST is expressed in most motor neurons (Fig. 2a).

We bred CAST Tg mice with hSOD1^{G93A} mice to produce hSOD1^{G93A}/CAST double Tg mice and their littermate controls (wild type, hSOD1^{G93A} and CAST Tg mice). Quantitative immunoblot analyses of total spinal cords extracts from these mice at 9 months confirmed

significantly reduced levels of MAP2, neurofilament proteins and p35 in hSOD1^{G93A} mice (Fig. 2b, g, i, m–p, $p<0.05$, one-way ANOVA, see Table 1). MAP2, p35 and neurofilament levels were significantly increased by overexpression of CAST in hSOD1^{G93A} mice (Fig 2b, g, i, m–o, one-way ANOVA, see Table 1) except for NF-H (Fig. 2p) and were modestly elevated in CAST Tg mice (Fig. 2g, i, $p<0.05$, one-way ANOVA, see Table 1), (Rao *et al.* 2008) since these proteins are calpain substrates and their levels are increased due to an inhibition of baseline calpain activity. Similarly, CAST overexpression in hSOD1^{G93A} mice restored to WT levels the abnormally increased levels of specific-calpain cleaved 150-kDa protein (Fig. 2b, c–d, $p<0.05$, one-way ANOVA, see Table 1), caspase-3 cleaved 120-kDa spectrin (Fig. 2b, e–f, $p<0.05$, one-way ANOVA, see Table 1), and TauC3 formation (Fig. 2b, 2h, $p<0.05$, one-way ANOVA, see Table 1). Calpain is also known to activate caspase-3 indirectly and CAST overexpression inhibits caspase-3 activity (Rao et al., 2008; 2014). Therefore, generation of caspase-3 cleaved tau (TauC3) is inhibited in CAST mice (Fig. 2h, one-way ANOVA, see Table 1) and similar results were also obtained from the brains of CAST Tg mice (Rao et al., 2008). Finally, the greatly reduced levels of p35 and increased p25 in hSOD1^{G93A} spinal cords were restored to WT values when CAST was overexpressed in hSOD1^{G93A} mice (Fig. 2b, I and k, $p<0.05$, one-way ANOVA, see Table 1).

hSOD1^{G93A} mice accumulate SOD1 oligomers in spinal cord (Fig. 2b, 2l, $p<0.05$), the formation of which was significantly inhibited by CAST overexpression (Fig. 2b, 2l, $p<0.05$, Student's t-test). Fewer oligomer species are visible in the Fig. 2b blot than in Fig. 1c due to a shorter blot exposure that enabled differences in oligomer levels between hSOD1^{G93A} and hSOD1^{G93A}/CAST Tg mice to be appreciated. Collectively, the foregoing data demonstrate that CAST overexpression in hSOD1^{G93A} mice blocks calpain activation and a calpain-dependent neurodegenerative cascade consisting of cytoskeletal protein breakdown, cdk5 over-activation, activation of caspase-3, and SOD1 oligomer formation.

CAST overexpression attenuates motor axon degeneration, delays disease onset, and increases survival of hSOD1^{G93A} mice

We performed ultrastructural morphometric analyses of motor axons in L5 spinal cord ventral roots of hSOD1^{G93A}/CAST double Tg mice, hSOD1^{G93A}, CAST and WT mice (Rao *et al.* 2014) at 3, 6 (disease onset) and 9 months of age. We detected no morphological changes in any of the genotypes at 3 months of age (Fig. 3a); however, by 6 months at the time of disease onset (see materials and methods), hSOD1^{G93A} mice had a significantly lower number of motor axons and this reduction was prevented by CAST over-expression ($p<0.05$, one way ANOVA, see Table 2) (Fig. 3c). By 9 months, axonal degeneration was extensive and total axon number was lowered more than 30% ($p<0.05$, one-way ANOVA, see Table 2) (Fig. 3d) in hSOD1^{G93A} mice. A more detailed analysis of caliber distributions revealed that the largest caliber axons were preferentially lost in hSOD1^{G93A} mice, consistent with evidence that this axonal population is selectively vulnerable in ALS mouse models and human ALS patients (Bruijn *et al.* 2004). In hSOD1^{G93A}/CAST mice, by comparison, the morphologies and numbers of motor axons at 6 months of age were comparable to those of WT mice. Furthermore, at 9 months hSOD1^{G93A}/CAST Tg mice had many fewer degenerating axon profiles (Fig. 3a) and greater numbers of surviving motor axons compared to hSOD1^{G93A} mice (Fig. 3d). Surviving axons in hSOD1^{G93A}/CAST Tg

mice were not significantly different in total number compared to those in WT and CAST Tg mice although a very high proportion of the surviving axons were small in caliber and large diameter axons were significantly reduced in size (Fig. 3f, $p<0.05$, one-way ANOVA) compared to hSOD1^{G93A} (Fig. 3f, $p<0.05$, One-way ANOVA, see Table 2). Increased number of axons in hSOD1^{G93A}/CAST mice compared to hSOD1^{G93A} mice is due to increased survival of large caliber axons that did not grow to become large axons. If only small caliber axons were preferentially survived due to CAST overexpression, we would have seen an increase in small caliber axons in CAST mice but there is no change in survival of small caliber axons in CAST mice compared to WT mice (Fig. 3e).

CAST Tg and WT mice lived for more than 2 years (>730 days, data not shown), hSOD1^{G93A} Tg mice survived on an average of 285 days or ~9.5 months (Fig. 4a, n=52), which is close to the reported survival of heterozygous hSOD1^{G93A} mice (G1del, see materials and methods animals section) (Alexander *et al.* 2004). There were no differences in survival between male and female hSOD1^{G93A} mice in our study in BL6 background as previously described (Acevedo-Arozena *et al.,* 2011). Overexpression of CAST in hSOD1^{G93A} Tg mice improved average survival to 348 days (22% increase in life span) (Fig. 4a, n=44) or 11.6 months, $p<0.05$, Student's t-test), an increase of more than 2 months (63 days) compared to hSOD1^{G93A} mice. Modified Kaplan-Meier survival plots revealed an increased survival of hSOD1^{G93A}/CAST mice compared to SOD1^{G93A} mice (Fig. 4b). Disease onset was delayed by 29% in hSOD1^{G93A}/CAST Tg mice. While disease onset averaged 193 days or 6.4 months in hSOD1^{G93A} mice (Fig. 4c, n=52) similar to previously reported values (Alexander *et al.* 2004), and CAST overexpression in hSOD1^{G93A} mice delayed disease onset to 249 days or 8.3 months (Fig. 4c, n=44, $p<0.05$, Student's t-test). Although CAST delayed disease onset significantly in hSOD1^{G93A}/CAST mice, it did not alter disease duration (Fig. 4d, $p=0.5$, Student's t-test). Rotarod analysis indicates no detectable difference between all the 4 groups of mice for motor performance at 3 months of age (Fig. 4e, ns-non significant); however, at 6 months of age, hSOD1^{G93A} mice showed significantly reduced performance (Fig. 4f, $p<0.05$, one-way ANOVA, see Table 3) compared to WT, CAST and hSOD1^{G93A}/CAST mice (Fig. 4f, $p<0.05$, one-way ANOVA, see Table 3). Even at 9 months, hSOD1^{G93A}/CAST mice performed significantly better in Rotarod studies compared to hSOD1^{G93A} mice (Fig. 4g, $p<0.05$, one-way ANOVA, see Table 3) indicating that overexpression of CAST in hSOD1^{G93A} mice substantially delayed a decline in motor performance. The better motor performance of the hSOD1^{G93A}/CAST mice compared to hSOD1^{G93A} mice implied that the surviving axons in the former mouse model, despite reductions in caliber, had relatively preserved function in the Rotorod task.

Discussion

Our results provide the first *in vivo* evidence that highly specific inhibition of calpains in neurons by CAST delays motor axon death and substantially extends lifespan in the hSOD1^{G93A} ALS mouse model (Dal Canto & Gurney 1997). The broad range of ameliorative effects of calpain inhibition support the conclusion that calpain over-activation is an early and critical event in the pathogenesis of at least this familial form of ALS. The extension of lifespan in hSOD1^{G93A}/CAST mice averaged at 63 days (22%), which is as good as or better than previous studies summarized in Table 4 (Williamson *et al.* 1998,

Kieran *et al.* 2005, Kieran *et al.* 2004, Roberts *et al.* 2014, Kong *et al.* 2014, Dadon-Nachum *et al.* 2015, Li *et al.* 2000). In earlier studies, hSOD1^{G93A} mice with a dynein motor protein mutation (*loa*) showed increased average survival of 35 days (28%) due to delayed disease progression (Kieran et al., 2005). Treatment of hSOD1^{G93A} mice with zVAD-fmk, which inhibits both caspase-1 and 3, led to an average increase in life span of 27 days (22%) (Li *et al.* 2000). Transplantation of a mixture of muscle progenitor cells expressing brain-derived neurotrophic factor, glial-derived neurotrophic factor, vesicular endothelial growth factor and insulin growth factor-1 resulted in an average delay of disease onset symptoms in hSOD1^{G93A} mice of 30 days and prolonged average life span by 13 days (Dadon-Nachum *et al.* 2015). Loss of NF-L from hSOD1^{G85R} mice led to an increase in average survival of 45 days (12%) due to delayed disease onset (Williamson *et al.* 1998). A small molecule activator of glutamate transporter EAAT2 translation (LDN/OSU-0212320) increased average survival of hSOD1^{G93A} mice by 15 days (Kong *et al.* 2014). Treatment of hSOD1^{G93A} mice with the heat shock protein co-inducer, arimoclomol, increased mean life span by delaying the disease progression by 28 days (22%) (Kieran *et al.* 2004). Overexpression of human copper uptake transporter 1 (hCTR1) led to a 12% increase in median survival time in hSOD1^{G37R} mice (Roberts *et al.* 2014). It should be noted, in this regard, that reliable comparisons are difficult because, in other studies, mutant hSOD1 expression of the models was higher and, in some cases, treatment was implemented near the time of disease onset or during progression rather than at an early postnatal age as done in our studies.

Our observations involving neuron-specific CAST expression are consistent with other reports indicating that disease initiates in neurons. In this regard, motor neuron specific overexpression of Thy-1.2 promoter driven mutant hSOD1^{G93A} produced motor neuron disease in mice (Jaarsma *et al.* 2008) and deletion of mutant hSOD1^{G37R} protein in motor neurons delayed disease onset (Boillee *et al.* 2006). Moreover the absence of an effect of neuronal CAST expression on disease progression accords with previous observations that deletion of mutant hSOD1^{G37R} protein from glial cells prolongs disease progression. Collectively, these findings suggest that disease onset is determined from the toxicity within motor neurons and disease progression is regulated partly by glial cells (Boillee *et al.* 2006). Our data establish a calpain activation-dependent pattern of biochemical changes in motor neurons including increased breakdown of various cytoskeletal proteins and activation of cdk5 and caspase-3, leading to extensive motor axon degeneration (Fig. 4h) in hSOD1^{G93A} mice. These data extend previous findings in high copy (~25) number hSOD1^{G93A} mice that calpain is activated in motor cortex and also in spinal cord as early as 30 days of age (Stifanese *et al.* 2014), and at 3 months earlier than the disease onset in our model highlights its early involvement in the disease process. Calpain activation, depletion of its endogenous inhibitor CAST, has been previously shown to induce a similar cascade of fibrillary degenerative events in AD brain and in mouse models of several other neurodegenerative disorders (Rao *et al.* 2008, Rao *et al.* 2014, Menzies *et al.* 2015, Diepenbroek *et al.* 2014), suggesting that the calpain-mediated cascade is potentially a key pathogenic mechanism and a common final pathway to neurodegeneration. It is also known that in dissociated spinal motor neuron cultures from hSOD1^{G93A} mice, CAST overexpression decreased numbers of inclusions and increased neuron viability *in vitro* (Tradewell & Durham 2010).

Recent evidence indicates that SOD1 oligomers play an important role in the degeneration of motor neurons in mutant mice. The therapies directed at reducing the burden of SOD1 oligomers in ALS mouse models increased the survival of mice (Liu et al., 2012; Nassif et al., 2014). It is known that mutant SOD1 enters mitochondria where the protein is oxidized to form oligomers. These SOD1 oligomers may interfere in mitochondrial oxidative phosphorylation or the electron transport chain to produce less ATP. Increased oxidation and nitrative stress in motor neurons may lead to activation of microglial cells to induce inflammation. Increased calcium in the cell leads to calpain activation to cleave nitric oxide synthase to induce oxidative stress (Stifanese *et al.* 2011). CAST is known to prevent oligomerization of Tau (Rao et al., 2014) and α-synuclein (Diepenbroek *et al.* 2014) and inhibit reactive gliosis (Rao et al., 2008). We speculate that CAST in $hSOD1^{G93A}$ mice may inhibit oxidative stress, thereby preventing oligomerization of hSOD1, preventing motor neuron degeneration and increasing the survival of mice.

Although our results establish a pathogenic role of calpains in $hSOD1^{G93A}$ mice, the antecedent events leading to abnormal calpain activation and a likely upstream dysregulation of calcium are unclear. Mutant SOD1 protein interferes with various cellular processes, including oxidative phosphorylation of mitochondria, endoplasmic reticulum stress, excitotoxicity, and protein oligomer formation or aggregation either causing, or secondary to, impairments of ubiquitin-proteasome (Ajroud-Driss & Siddique 2015) and autophagy (Nassif *et al.* 2014) function. Multiple studies have indicated that calpains are activated in ALS, Cdk5 activator protein p35 is cleaved by calpain to produce p25 that constitutes deregulated Cdk5 enzyme in human ALS patients as well as in mouse models of ALS (Klinman and Holzbaur, 2015) to promote neurodegeneration (Fig. 4h). Calpain is known to cleave inhibitor kappa B-alpha (Scholzke *et al.* 2003), atg5 (Yousefi *et al.* 2006), and TAR DNA Binding protein-43 (Yamashita *et al.* 2012) to promote neurodegeneration. Calpains are also known to execute neuronal cell death through activation of multiple caspases or in a caspase-independent manner (Cabon *et al.* 2012). All of these mechanisms are potential underlying contributions to calcium dysregulation and calpain activation (Tadic *et al.* 2014). Importantly, our results and those in other studies indicate that, regardless of the number of distinct mechanisms by which calpains are activated in different neurological disorders, inhibition of these proteases by CAST has striking ameliorative effects on disease development and overall survival.

Multiple synthetic inhibitors of calpain have been used to prevent calpain hyperactivation in cell and animal models and, in many cases, have attenuated calpain-mediated cell dysfunction and neurodegeneration (Nixon 2003, Trinchese *et al.* 2008). Synthetic inhibitors of calpain, however, inhibit other cysteine proteases, including cathepsins, and in some cases, serine proteinases. CAST remains the only truly specific inhibitor of calpains (Goll *et al.* 2003) and a more complete understanding of CAST structure and regulation will be crucial to the development of CAST mimetics and other highly specific calpain inhibitors to prevent or delay the development of motor neuron disease.

Acknowledgments

hSOD1^{G93A} low expression line of mice (SOD1*G93Adl)1Gur (SOD1G93Adl; also known as G1del) was a kind gift of Dr. Zhuoshang Xu (University of Massachussetts, Worcester, MA). This work is funded by National Institutes of Health/National Institute on Neurological Diseases Aging: 5R21NS61190-2 (M.V.R), National Institute on Aging: PO1AG017617 (R.A.N) and RO1AG005604 (R.A.N and M.V.R). We would like to thank Philip H. Stavrides for capturing IHC images and Nicole Gogel for formatting the paper for publication.

Abbreviations

hSOD1	human superoxide dismutase 1
ALS	amyotrophic lateral sclerosis
CAST	calpastatin
Cal I	calpain I
Cal II	calpain II

References

Acevedo-Arozena A, Kalmar B, Essa S, Ricketts T, Joyce P, Kent R, Rowe C, Parker A, Gray A, Hafezparast M, Thorpe JR, Greensmith L, Fisher EM. A comprehensive assessment of the SOD1G93A low-copy transgenic mouse, which models human amyotrophic lateral sclerosis. Dis Model Mech. 2011; 4:686–700. [PubMed: 21540242]

Ajroud-Driss S, Siddique T. Sporadic and hereditary amyotrophic lateral sclerosis (ALS). Biochim Biophys Acta. 2015; 1852:679–684. [PubMed: 25193032]

Alexander GM, Erwin KL, Byers N, Deitch JS, Augelli BJ, Blankenhorn EP, Heiman-Patterson TD. Effect of transgene copy number on survival in the G93A SOD1 transgenic mouse model of ALS. Brain Res Mol Brain Res. 2004; 130:7–15. [PubMed: 15519671]

Andersen PM, Al-Chalabi A. Clinical genetics of amyotrophic lateral sclerosis: what do we really know? Nat Rev Neurol. 2011; 7:603–615. [PubMed: 21989245]

Boillee S, Yamanaka K, Lobsiger CS, Copeland NG, Jenkins NA, Kassiotis G, Kollias G, Cleveland DW. Onset and progression in inherited ALS determined by motor neurons and microglia. Science. 2006; 312:1389–1392. [PubMed: 16741123]

Bosco DA, Morfini G, Karabacak NM, et al. Wild-type and mutant SOD1 share an aberrant conformation and a common pathogenic pathway in ALS. Nat Neurosci. 2010; 13:1396–1403. [PubMed: 20953194]

Boston-Howes W, Gibb SL, Williams EO, Pasinelli P, Brown RH Jr, Trotti D. Caspase-3 cleaves and inactivates the glutamate transporter EAAT2. J Biol Chem. 2006; 281:14076–14084. [PubMed: 16567804]

Bruijn LI, Miller TM, Cleveland DW. Unraveling the mechanisms involved in motor neuron degeneration in ALS. Annu Rev Neurosci. 2004; 27:723–749. [PubMed: 15217349]

Cabon L, Galan-Malo P, Bouharrour A, Delavallee L, Brunelle-Navas MN, Lorenzo HK, Gross A, Susin SA. BID regulates AIF-mediated caspase-independent necroptosis by promoting BAX activation. Cell Death Differ. 2012; 19:245–256. [PubMed: 21738214]

Dadon-Nachum M, Ben-Yaacov K, Ben-Zur T, Barhum Y, Yaffe D, Perlson E, Offen D. Transplanted modified muscle progenitor cells expressing a mixture of neurotrophic factors delay disease onset and enhance survival in the SOD1 mouse model of ALS. J Mol Neurosci. 2015; 55:788–797. [PubMed: 25330859]

Dal Canto MC, Gurney ME. A low expressor line of transgenic mice carrying a mutant human Cu,Zn superoxide dismutase (SOD1) gene develops pathological changes that most closely resemble those in human amyotrophic lateral sclerosis. Acta Neuropathol. 1997; 93:537–550. [PubMed: 9194892]

Diepenbroek M, Casadei N, Esmer H, et al. Overexpression of the calpain-specific inhibitor calpastatin reduces human alpha-Synuclein processing, aggregation and synaptic impairment in [A30P]alphaSyn transgenic mice. Hum Mol Genet. 2014; 23:3975–3989. [PubMed: 24619358]

Doble A. The pharmacology and mechanism of action of riluzole. Neurology. 1996; 47:S233–241. [PubMed: 8959995]

Furman JL, Norris CM. Calcineurin and glial signaling: neuroinflammation and beyond. J Neuroinflammation. 2014; 11:158. [PubMed: 25199950]

Geddes JW, Saatman KE. Targeting individual calpain isoforms for neuroprotection. Exp Neurol. 2010; 226:6–7. [PubMed: 20682310]

Goll DE, Thompson VF, Li H, Wei W, Cong J. The calpain system. Physiol Rev. 2003; 83:731–801. [PubMed: 12843408]

Grynspan F, Griffin WR, Cataldo A, Katayama S, Nixon RA. Active site-directed antibodies identify calpain II as an early-appearing and pervasive component of neurofibrillary pathology in Alzheimer's disease. Brain Res. 1997; 763:145–158. [PubMed: 9296555]

Gurney ME, Pu H, Chiu AY, et al. Motor neuron degeneration in mice that express a human Cu,Zn superoxide dismutase mutation. Science. 1994; 264:1772–1775. [PubMed: 8209258]

Higuchi M, Iwata N, Matsuba Y, et al. Mechanistic involvement of the calpain-calpastatin system in Alzheimer neuropathology. FASEB J. 2012; 26:1204–1217. [PubMed: 22173972]

Jaarsma D, Teuling E, Haasdijk ED, De Zeeuw CI, Hoogenraad CC. Neuron-specific expression of mutant superoxide dismutase is sufficient to induce amyotrophic lateral sclerosis in transgenic mice. J Neurosci. 2008; 28:2075–2088. [PubMed: 18305242]

Klinman E, Holzbaur EL. Stress-Induced CDK5 Activation Disrupts Axonal Transport via Lis1/Ndel1/Dynein. Cell Rep. 2015; 12:462–73. [PubMed: 26166569]

Kieran D, Hafezparast M, Bohnert S, Dick JR, Martin J, Schiavo G, Fisher EM, Greensmith L. A mutation in dynein rescues axonal transport defects and extends the life span of ALS mice. J Cell Biol. 2005; 169:561–567. [PubMed: 15911875]

Kieran D, Kalmar B, Dick JR, Riddoch-Contreras J, Burnstock G, Greensmith L. Treatment with arimoclomol, a coinducer of heat shock proteins, delays disease progression in ALS mice. Nat Med. 2004; 10:402–405. [PubMed: 15034571]

Kong Q, Chang LC, Takahashi K, et al. Small-molecule activator of glutamate transporter EAAT2 translation provides neuroprotection. J Clin Invest. 2014; 124:1255–1267. [PubMed: 24569372]

Li M, Ona VO, Guegan C, et al. Functional role of caspase-1 and caspase-3 in an ALS transgenic mouse model. Science. 2000; 288:335–339. [PubMed: 10764647]

Liu HN, Tjostheim S, Dasilva K, et al. Targeting of monomer/misfolded SOD1 as a therapeutic strategy for amyotrophic lateral sclerosis. J Neurosci. 2012; 32:8791–8799. [PubMed: 22745481]

McBrayer M, Nixon RA. Lysosome and calcium dysregulation in Alzheimer's disease: partners in crime. Biochem Soc Trans. 2013; 41:1495–1502. [PubMed: 24256243]

Menzies FM, Garcia-Arencibia M, Imarisio S, et al. Calpain inhibition mediates autophagy-dependent protection against polyglutamine toxicity. Cell Death Differ. 2015; 22:433–444. [PubMed: 25257175]

Nassif M, Valenzuela V, Rojas-Rivera D, et al. Pathogenic role of BECN1/Beclin 1 in the development of amyotrophic lateral sclerosis. Autophagy. 2014; 10:1256–1271. [PubMed: 24905722]

Nguyen MD, Julien JP. Cyclin-dependent kinase 5 in amyotrophic lateral sclerosis. Neurosignals. 2003; 12:215–220. [PubMed: 14673208]

Nixon RA. The calpains in aging and aging-related diseases. Ageing Res Rev. 2003; 2:407–418. [PubMed: 14522243]

Rao MV, McBrayer MK, Campbell J, et al. Specific calpain inhibition by calpastatin prevents tauopathy and neurodegeneration and restores normal lifespan in tau P301L mice. J Neurosci. 2014; 34:9222–9234. [PubMed: 25009256]

Rao MV, Mohan PS, Peterhoff CM, et al. Marked calpastatin (CAST) depletion in Alzheimer's disease accelerates cytoskeleton disruption and neurodegeneration: neuroprotection by CAST overexpression. J Neurosci. 2008; 28:12241–12254. [PubMed: 19020018]

Ray SK, Wilford GG, Ali SF, Banik NL. Calpain upregulation in spinal cords of mice with 1-methyl-4-phenyl-1,2,3,6-tetrahydropyridine (MPTP)-induced Parkinson's disease. Ann N Y Acad Sci. 2000; 914:275–283. [PubMed: 11085327]

Reaume AG, Elliott JL, Hoffman EK, et al. Motor neurons in Cu/Zn superoxide dismutase-deficient mice develop normally but exhibit enhanced cell death after axonal injury. Nat Genet. 1996; 13:43–47. [PubMed: 8673102]

Robberecht W, Philips T. The changing scene of amyotrophic lateral sclerosis. Nat Rev Neurosci. 2013; 14:248–264. [PubMed: 23463272]

Roberts BR, Lim NK, McAllum EJ, et al. Oral treatment with Cu(II)(atsm) increases mutant SOD1 in vivo but protects motor neurons and improves the phenotype of a transgenic mouse model of amyotrophic lateral sclerosis. J Neurosci. 2014; 34:8021–8031. [PubMed: 24899723]

Rosen DR, Siddique T, Patterson D, et al. Mutations in Cu/Zn superoxide dismutase gene are associated with familial amyotrophic lateral sclerosis. Nature. 1993; 362:59–62. [PubMed: 8446170]

Scholzke MN, Potrovita I, Subramaniam S, Prinz S, Schwaninger M. Glutamate activates NF-kappaB through calpain in neurons. Eur J Neurosci. 2003; 18:3305–3310. [PubMed: 14686903]

Spencer MJ, Mellgren RL. Overexpression of a calpastatin transgene in mdx muscle reduces dystrophic pathology. Hum Mol Genet. 2002; 11:2645–2655. [PubMed: 12354790]

Stifanese R, Averna M, Pedrazzi, De Tullio R, Salamino F, Pontremoli S, Melloni E. Is the expression of [-G93A(+)] human SOD1 a model to study neurodegenerations. J Biol Res. 2011; 84:1.

Stifanese R, Averna M, De Tullio R, et al. Role of calpain-1 in the early phase of experimental ALS. Arch Biochem Biophys. 2014; 562:1–8. [PubMed: 25151305]

Tadic V, Prell T, Lautenschlaeger J, Grosskreutz J. The ER mitochondria calcium cycle and ER stress response as therapeutic targets in amyotrophic lateral sclerosis. Front Cell Neurosci. 2014; 8:147. [PubMed: 24910594]

Thapa A, Morris L, Xu J, Ma H, Michalakis S, Biel M, Ding XQ. Endoplasmic reticulum stress-associated cone photoreceptor degeneration in cyclic nucleotide-gated channel deficiency. J Biol Chem. 2012; 287:18018–18029. [PubMed: 22493484]

Tradewell ML, Durham HD. Calpastatin reduces toxicity of SOD1G93A in a culture model of amyotrophic lateral sclerosis. Neuroreport. 2010; 21:976–979. [PubMed: 20736867]

Trinchese F, Fa M, Liu S, et al. Inhibition of calpains improves memory and synaptic transmission in a mouse model of Alzheimer disease. J Clin Invest. 2008; 118:2796–2807. [PubMed: 18596919]

Van Den Bosch L, Van Damme P, Bogaert E, Robberecht W. The role of excitotoxicity in the pathogenesis of amyotrophic lateral sclerosis. Biochim Biophys Acta. 2006; 1762:1068–1082. [PubMed: 16806844]

Wang KK, Posmantur R, Nadimpalli R, et al. Caspase-mediated fragmentation of calpain inhibitor protein calpastatin during apoptosis. Arch Biochem Biophys. 1998; 356:187–196. [PubMed: 9705209]

Williamson TL, Bruijn LI, Zhu Q, Anderson KL, Anderson SD, Julien JP, Cleveland DW. Absence of neurofilaments reduces the selective vulnerability of motor neurons and slows disease caused by a familial amyotrophic lateral sclerosis-linked superoxide dismutase 1 mutant. Proc Natl Acad Sci U S A. 1998; 95:9631–9636. [PubMed: 9689132]

Wootz H, Hansson I, Korhonen L, Lindholm D. XIAP decreases caspase-12 cleavage and calpain activity in spinal cord of ALS transgenic mice. Exp Cell Res. 2006; 312:1890–1898. [PubMed: 16566922]

Yamashita T, Hideyama T, Hachiga K, Teramoto S, Takano J, Iwata N, Saido TC, Kwak S. A role for calpain-dependent cleavage of TDP-43 in amyotrophic lateral sclerosis pathology. Nat Commun. 2012; 3:1307. [PubMed: 23250437]

Yousefi S, Perozzo R, Schmid I, Ziemiecki A, Schaffner T, Scapozza L, Brunner T, Simon HU. Calpain-mediated cleavage of Atg5 switches autophagy to apoptosis. Nat Cell Biol. 2006; 8:1124–1132. [PubMed: 16998475]

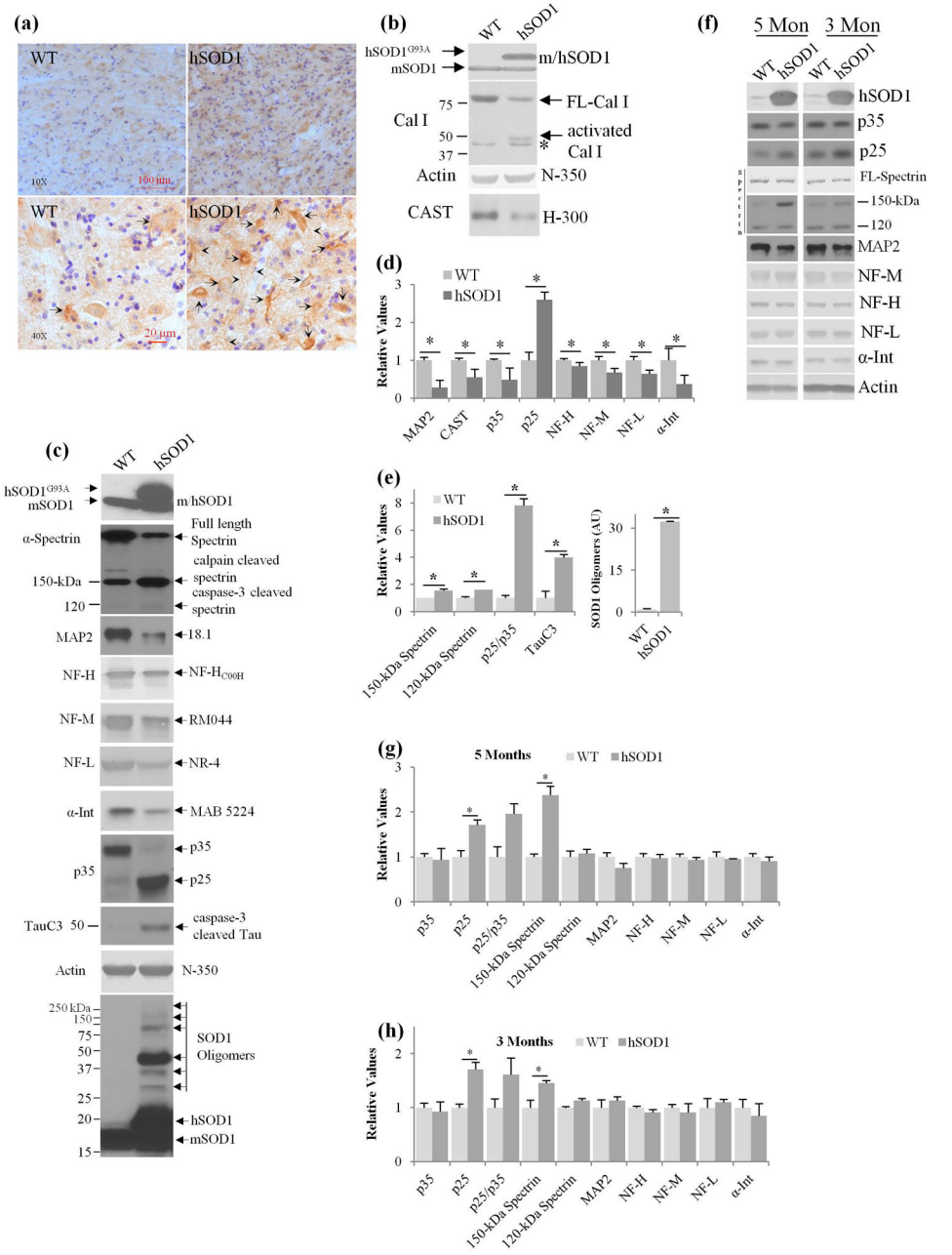

Fig. 1.

Calpain activation and CAST depletion in hSOD1^{G93A} spinal cords. End stage hSOD1^{G93A} mice (~9 month old) and their age matched wild type (WT) spinal cord sections were immunostained with Cal II activation site specific polyclonal antibody [C-24, (Rao *et al.* 2014, Rao *et al.* 2008)] Fig. 1a, at 10x, and 40x, C-24 (see arrows for neuronal cell bodies and arrow heads for neuronal processes staining, DAB stain, -brown, cresyl violet for nuclear stain, -blue) and the spinal cord extracts from the similar mice were immunoblotted with Cal I (b), actin (N-350) and CAST (B, H-300) antibodies. Nonspecific band in B for Cal I immunoblot is indicated with an asterisk (*). (c) Calpain-mediated cytoskeletal protein

breakdown in hSOD1^{G93A} spinal cords. Spinal cord extracts from end stage mice (as indicated above) were immunoblotted with SOD1 (human/mouse), α-spectrin, MAP2, NF subunit proteins, p35, TauC3, and actin antibodies indicate increased calpain cleaved 150-kDa spectrin breakdown product, 120-kDa caspase-3 cleaved product, reduced MAP2, increased production of p25, increased TauC3 formation and increased formation of SOD1 oligomers were observed in hSOD1^{G93A} mice while the levels of actin was unaltered. Phosphorylated and glycosylated proteins appear on immunoblots as relatively diffuse bands. Neurofilament and spectrin proteins are also phosphorylated and glycosylated, as a result immunoreactive bands of these proteins appear as relatively diffuse bands. The bands of interest for quantification of these proteins are indicated with an arrow in Fig. 1. (d–e) Quantification of MAP2, CAST, P35, P25, NF-H, NF-M, NF-L, α-Internexin, 150-kDa spectrin, 120-kDa spectrin, p25/p35 ratio, TauC3 and SOD1 oligomers from spinal cords of end stage hSOD1^{G93A} mice (~9 months) and age matched WT mice (n=3–6 mice for each genotype). (f–h) Immunoblot analysis of spinal cord extracts of hSOD1^{G93A} mice at 3 and 5 months of age (f), quantification of P35, P25, p25/p35 ratio, 150-kDa spectrin, 120-kDa spectrin, MAP2, NF-H, NF-M, NF-L, α-Internexin at 5 months (g) and 3 months (h) of age in hSOD1^{G93A} mice. *- $P<0.05$ is significant; for all panels in Fig. 1 Student's t-test is employed.

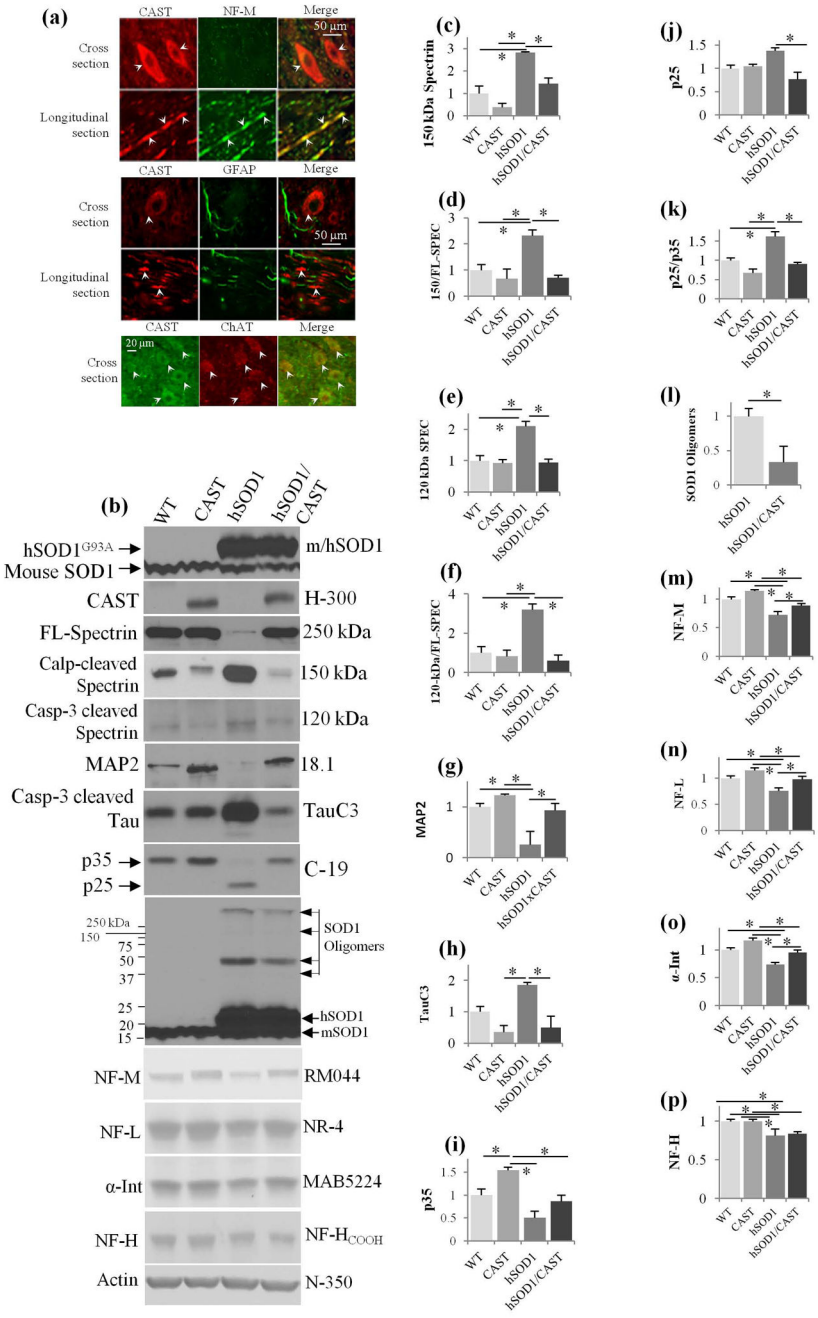

Fig. 2.

Neuron specific expression of CAST under Thy-1-promoter in spinal cords of CAST Tg mice inhibits cytoskeletal protein breakdown, CDK5 activation and SOD1 oligomerization in hSOD1^{G93A} mice spinal cords. (a) Spinal cord sections (cross and longitudinal sections) form CAST Tg mice were double immunostained with CAST 3.1 (CAST) and RM044 (NF-M, neuron specific) antibodies or CAST 3.1 and GFAP (glial specific) or CAST 3.1 and ChAT (motor neuron specific) antibodies. CAST Tg mice spinal cords exhibited colocalization of CAST with NF-M in neuron specific and ChAT motor neuron specific manner but not with GFAP. (b) Spinal cord extracts from (9 month old) mice of hSOD1^{G93A}

mice, WT, CAST and hSOD1^{G93A}/CAST mice were immunoblotted with SOD1 (human/mouse), CAST, spectrin, MAP2, TauC3, p35, NF-M, NF-L, α-Internexin, and NF-H antibodies. (c–p) Quantification of 150-kDa calpain cleaved spectrin (c), the ratio of 150/FL-spectrin (d), 120-kDa caspase-3 cleaved spectrin (e), 120-kDa/FL-spectrin ratio (f), MAP2 (g), TauC3 (h), p35 (i), p25 (j), p25/p35 (k), SOD1 oligomers (l), NF-M (m), NF-L (n), α-Internexin (o) and NF-H (Fig. 2p) in WT, CAST, hSOD1^{G93A} and hSOD1^{G93A}/CAST mice. *- $p<0.05$ is significant. For panels in Fig. 2c–k, m–p: One-way ANOVA and for panel- l: Student's t-test is employed.

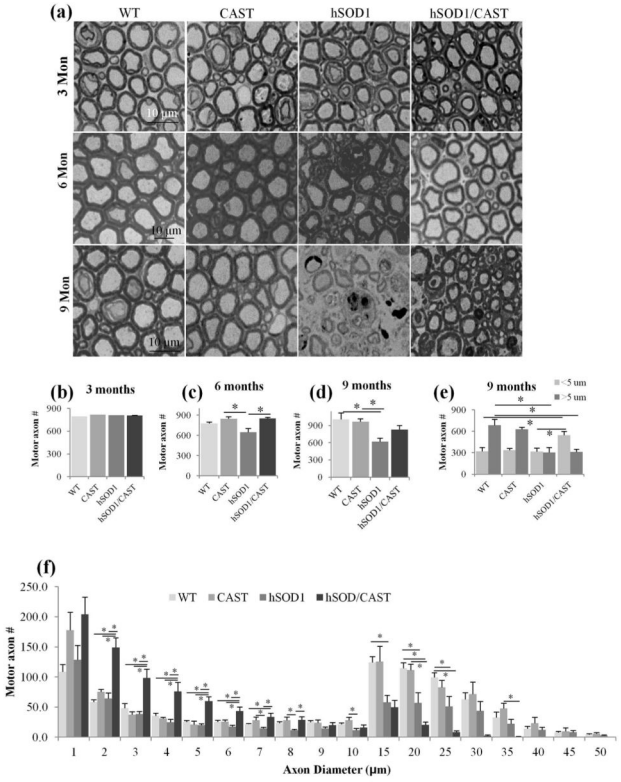

Fig. 3.

Overexpression of CAST in hSOD1^{G93A} motor neurons increases the survival of motor axons. Mice were perfused (glutaraldehyde/paraformaldehyde) at 3, 6 and 9 months of age, L5 ventral roots were dissected from WT, CAST, hSOD1^{G93A} mice and hSOD1^{G93A}/CAST mice, whole root was imaged, axon diameters were measured using Bioquant and axons were grouped into 2 sizes (<5 μm and more than 5 μm). (a) Axonal profiles of WT, CAST, hSOD1^{G93A} and hSOD1^{G93A}/CAST mice at 3, 6 and 9 months of age. Overexpression of CAST in hSOD1^{G93A} mice did not alter the survival of motor axons at 3 months of age (a and b) but significantly increased survival at 6 months (a and c, $p<0.05$, one-way ANOVA), and 9 months of age (a and d). Grouping of axons in to small caliber (<5 μm) and large caliber (>5 μm) demonstrates CAST overexpression significantly increased the survival of small caliber axons sizes (<5 μm, Fig. 3e, $p<0.05$, one-way ANOVA). (f) Caliber distribution of axons from WT, CAST, hSOD1^{G93A} and hSOD1^{G93A}/CAST mice indicate depletion of large caliber axons (>5 um) in hSOD1^{G93A} mice, and however there is a significant increase in survival of small caliber axons in hSOD1^{G93A}/CAST mice (Fig. 3f, $p<0.05$, one-way ANOVA). For all panels in Fig. 3 One-way ANOVA is employed.

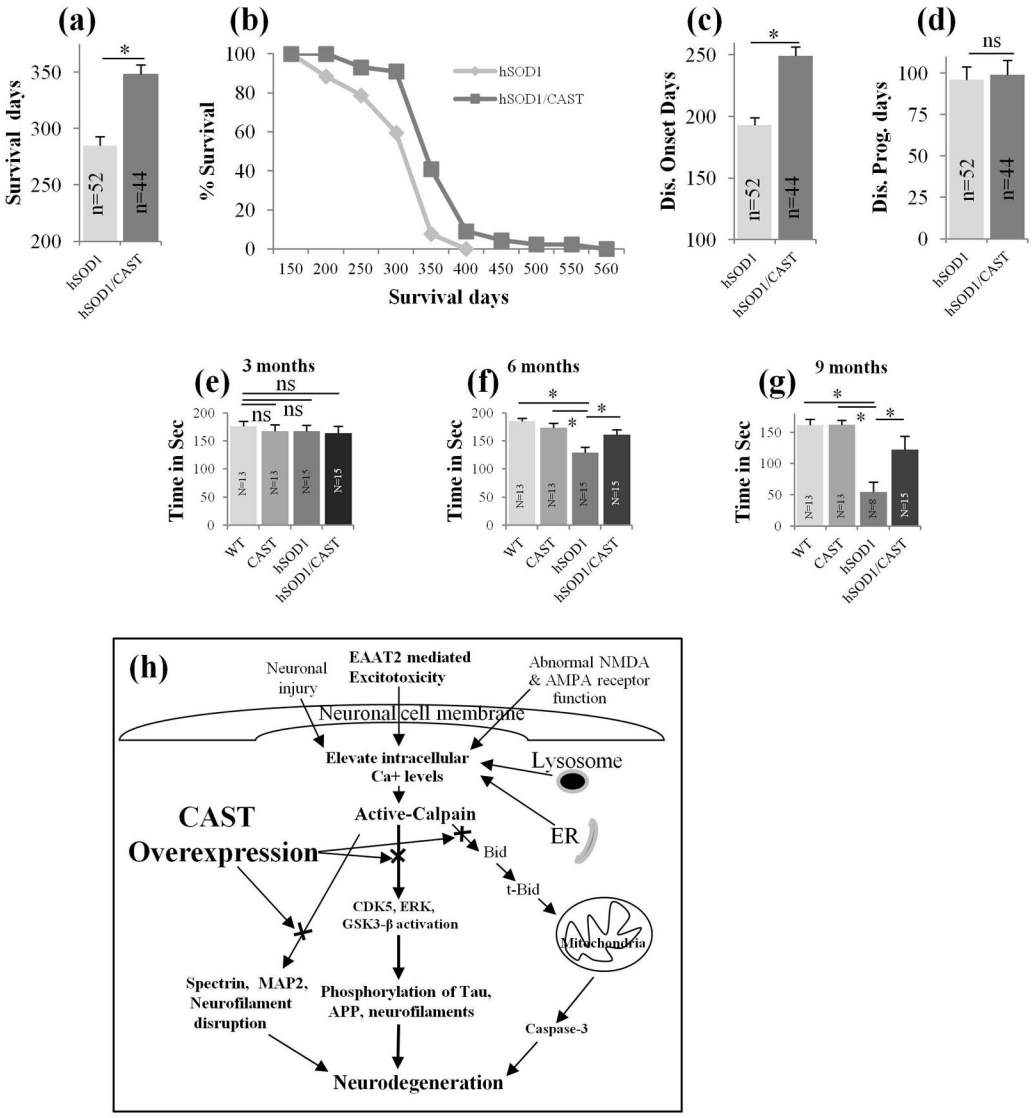

Fig. 4.

CAST overexpression in hSOD1^{G93A} motor neurons prolongs survival of the mice by delaying the disease onset. SOD1/CAST double Tg mice survive significantly longer (2 months, a, $p<0.05$; Student's t-test) compared to hSOD1^{G93A} mice (data pooled from male and female mice, n=52 for hSOD1^{G93A} mice; n=44 for hSOD1^{G93A}/CAST mice, WT and CAST mice lived for more than 2 years, data not shown). Modified Kaplan-Meier curves also indicate increased survival of hSOD1^{G93A}/CAST mice compared to hSOD1^{G93A} mice (b, the number of the mice for b is same as in Fig. 4a). Overexpression of CAST in hSOD1^{G93A} mice delayed disease onset by 2 months (c, n=52 for hSOD1^{G93A} mice; n=44 for hSOD1^{G93A}/CAST mice, $p<0.05$; Student's t-test) while CAST did not have a significant effect on disease duration in hSOD1^{G93A} mice (d, n=52 for hSOD1^{G93A}; n=44 for hSOD1^{G93A}/CAST mice; p=0.5; Student's t-test). (e–g) Rotarod tests at 3 (e), 6 (f) and 9 months (g) were carried out and hSOD1^{G93A}/CAST Tg mice showed significantly improved motor performance at 6 (e, $p<0.05$, one-way ANOVA) and 9 months (g, $p<0.05$, one-way

ANOVA) of age compared to hSOD1^{G93A} mice, ns-non significant; *- P<0.05 is significant. In Fig. 4 for panel's a–d, Student's t-test and in Fig. 4e–g One-way ANOVA is employed. (h) A model depicting activation of calpain in ALS mouse model and inhibition of activated calpain with CAST prevents cytoskeletal protein breakdown, activation of Cdk5 and cleavage of Cam Kinase IV to prevent neurodegeneration. Abnormally high calcium imbalance in ALS and its mouse models at mitochondria, endoplasmic reticulum (Tadic *et al.* 2014), lysosomes (McBrayer & Nixon 2013), excitotoxicity (Van Den Bosch *et al.* 2006, Tadic *et al.* 2014), abnormal NMDA and AMPA receptor function (Van Den Bosch *et al.* 2006, Tadic *et al.* 2014), neuronal injury (spinal cord and traumatic brain injury) (Geddes & Saatman 2010) results in activation of calpain and depletion of CAST in neurons (Rao *et al.* 2014, Rao *et al.* 2008). Activated calpain leads to cascade of events to initiate activation of Cdk5 (cleaves p35 to p25 to produce constitutively active enzyme), Erk1/2, GSK3beta to pathologically phosphorylate Tau, neurofilaments to initiate neurotoxic mechanisms. Activated calpain also can initiate breakdown of NFs, tau, MAPs, spectrin, Cam Kinase IV and calcineurin A to destabilize neuronal cytoskeletal and loss of synapses to cause neurodegeneration (Rao *et al.* 2014, Rao *et al.* 2008, Furman & Norris 2014). Calpain also can indirectly activate caspase-3 by cleaving Bid to produce truncated-Bid, resulting in the depolarization of the mitochondrial membrane (Cabon *et al.* 2012), release of cytochrome C, activation of caspase-3, and ultimately apoptosis-mediated neuronal cell death. Restoration of depleted CAST levels in an ALS mouse model by overexpression of CAST prevents the above cascade of neurotoxic mechanisms to delay disease onset and prolong life span of these mice.

Table 1

One-way ANOVA values for Proteins used in Fig. 2.

Protein	DF values	p values
Fig. 2c 150-kDa Spectrin	F (3, 20) = 8.901	P = 0.0006
Fig. 2d 150 to FL Spectrin	F (3, 20) = 8.569	P = 0.0007
Fig. 2e 120-kDa Spectrin	F (3, 32) = 14.26	P < 0.0001
Fig. 2f 120 to FL Spectrin	F (3, 32) = 5.502	P = 0.0037
Fig. 2g MAP2	F (3, 8) = 25.07	P = 0.0002
Fig. 2h TauC3	F (3, 10) = 9.057	P = 0.0034
Fig. 2i p35	F (3, 26) = 12.25	P < 0.0001
Fig. 2j p25	F (3, 26) = 5.747	P = 0.0037
Fig. 2k p25/935	F (3, 26) = 12.87	P < 0.0001
Fig. 2m NF-M	F (3, 27) = 22.70	P < 0.0001
Fig. 2n NF-L	F (3, 25) = 28.83	P < 0.0001
Fig. 2o α-Internexin	F (3, 28) = 15.64	P < 0.0001
Fig. 2p NF-H	F (3, 35) = 21.77	P < 0.0001

Table 2

One way ANOVA values for Fig. 3.

	DF values	p values
Fig. 3b Motor Axons at 3 months	F (3, 26) = 0.3325	P = 0.8019
Fig. 3c Motor Axons at 6 months	F (3, 16) = 4.703	P = 0.0154
Fig. 3d Motor Axons at 9 months	F (3, 24) = 5.635	P = 0.0045
Fig. 3e Motor Axons at 9 months < 5 μm	F (3, 16) = 4.260	P = 0.0216
Fig. 3e Motor Axons at 9 months > 5 μm	F (3, 16) = 7.336	P = 0.0026
Fig. 3f Motor axon Bin 1 μm	F (3, 15) = 0.6916	P = 0.5713
Fig. 3f Motor axon Bin 2 μm	F (3, 15) = 7.284	P = 0.0031
Fig. 3f Motor axon Bin 3 μm	F (3, 15) = 11.27	P = 0.0004
Fig. 3f Motor axon Bin 4 μm	F (3, 15) = 10.10	P = 0.0007
Fig. 3f Motor axon Bin 5 μm	F (3, 15) = 27.57	P < 0.0001
Fig. 3f Motor axon Bin 6 μm	F (3, 15) = 9.998	P = 0.0007
Fig. 3f Motor axon Bin 7 μm	F (3, 15) = 12.49	P = 0.0002
Fig. 3f Motor axon Bin 8 μm	F (3, 15) = 7.524	P = 0.0027
Fig. 3f Motor axon Bin 9 μm	F (3, 15) = 2.373	P = 0.1112
Fig. 3f Motor axon Bin 10 μm	F (3, 15) = 3.501	P = 0.0419
Fig. 3f Motor axon Bin 15 μm	F (3, 15) = 5.950	P = 0.0070
Fig. 3f Motor axon Bin 20 μm	F (3, 15) = 8.670	P = 0.0014
Fig. 3f Motor axon Bin 25 μm	F (3, 15) = 7.631	P = 0.0025
Fig. 3f Motor axon Bin 30 μm	F (3, 15) = 3.243	P = 0.0519
Fig. 3f Motor axon Bin 35 μm	F (3, 15) = 3.959	P = 0.0290
Fig. 3f Motor axon Bin 40 μm	F (3, 15) = 1.475	P = 0.2613
Fig. 3f Motor axon Bin 45 μm	F (3, 15) = 0.8952	P = 0.4664
Fig. 3f Motor axon Bin 50 μm	F (3, 15) = 1.685	P = 0.2129

Table 3

One way ANOVA values for Fig. 4.

	DF values	p values
Fig. 4e Rotarod at 3 months	F (3, 64) = 0.2790	P = 0.8403
Fig. 4f Rotarod at 6 months	F (3, 50) = 7.435	P = 0.0003
Fig. 4g Rotarod at 9 months	F (3, 41) = 7.632	P = 0.0004

Table 4

Survival times in days

	Survival		
Studies	**Average in days**	**Average %**	**Median %**
Rao et al.,(Current study)	63	22	11.9
Kieran et al., 2005	35	28	-
Li et al., 2000	27	22	-
Dadon-Nachum et al., 2015	13	9.4	-
Williamson et al., 1998	45	12	-
Kong et al., 2014	14.3	11.3	-
Kieran et al., 2004	28	22	-
Roberts et al., 2014	-	-	12